MCSCF and CASPT2N Calculations on the Excited States of 1,2,4,5-Tetramethylenebenzene. The UV–Vis Spectrum Observed Belongs to the Singlet State of the Diradical

David A. Hrovat and Weston Thatcher Borden*

Contribution from the Department of Chemistry, University of Washington, Seattle, Washington 98195

*Received February 14, 1994. Revised Manuscript Received April 8, 1994**

Abstract: CASSCF and CASPT2N calculations with the 6-31G* basis set have been performed in order to understand the UV–vis spectrum that has been observed for **TMB**. The calculations lead to the assignment of the $1^1A_g \rightarrow 2^1A_g$ transition as being responsible for the longest wavelength absorption in the spectrum. The nature of the 2^1A_g excited state is discussed. The CASPT2N excitation energies calculated for the four excited singlet states of lowest energy are in excellent agreement with those observed. This agreement provides evidence that the 1^1A_g state of **TMB** is responsible for the UV–vis spectrum. Therefore, our results confirm that, as predicted theoretically and as found by the experiments of Berson and co-workers, this disjoint diradical has a singlet ground state and, thus, violates Hund's rule.

Because the two nonbonding (NB) MOs of 1,2,4,5-tetramethylenebenzene (**TMB**) can be chosen so that they are disjoint (i.e., have no atoms in common), a singlet ground state is predicted for this diradical by qualitative MO theory.[1,2] Both semiempirical[3] and *ab initio*[4,5] calculations predict that **TMB** should have a singlet ground state and, thus, violate Hund's rule.[6,7] Nevertheless, the first experiments that were performed on **TMB** indicated a triplet ground state for this diradical.[8]

Evidence that, when the diradical was prepared in an argon matrix, the state of **TMB** observed was the triplet consisted of a triplet EPR spectrum and a long-wavelength absorption in the UV–vis spectrum. This absorption consisted of several weak vibrational bands, extending from slightly above 600 nm to about 530 nm, followed by a strong, unstructured absorption, centered at about 475 nm. A weak absorption, followed by a strong absorption at shorter wavelengths, had been predicted for the lowest triplet state of **TMB**, but *not for the lowest singlet*.[5]

Subsequent experiments by Berson and his collaborators[9] have established the following facts about **TMB**: (1) the EPR spectrum does not belong to **TMB**, but (2) the absorptions at 475 and 530–600 nm do; and (3) the state being observed is a singlet, which is apparently the ground state of **TMB**. Thus, while both qualitative[1,2] and more quantitative[3–5] theory correctly predict the ground state of **TMB**, the *ab initio* CI calculations that were performed in order to predict the UV–vis spectrum of this state[5] apparently failed to give even a qualitatively correct description of the spectrum. Berson, with characteristic charity, has written, "In our view the calculations at this time raise more questions than they answer.... We cannot rely upon the available computational results on the optical spectra as diagnostic for the spin of the ground state."[9c]

The failure of the previous CI calculations to predict correctly the UV–vis spectrum of singlet **TMB** is certainly regrettable, but it is also not surprising. The calculations included only correlation among the π electrons and used the same frozen wave function for the σ electrons in the calculations for all the excited states. Although it was noted that correlation between σ and π electrons would tend to selectively stabilize excited states with large amounts of ionic character,[5] the computational resources that were available at the time the calculations were carried out precluded the simultaneous inclusion of both π–π and σ–π electron correlation for a molecule the size of **TMB**.

During the eight years since the original calculations were performed, advances in computer hardware and in the software for *ab initio* calculations have made it possible to carry out much better calculations. Performing better calculations on the UV–vis spectrum of **TMB** is important for two reasons. First, although the experimental evidence for a singlet ground state for **TMB** seems unassailable,[9] the continued failure of calculations to explain the longest wavelength absorption in the UV–vis spectrum of **TMB** would raise the nagging doubt that perhaps this spectrum belonged to the lowest triplet, rather than to the lowest singlet state. Second, if, as claimed,[7,9] **TMB** is, in fact, the first non-Kekulé hydrocarbon diradical that has been found to violate Hund's rule, it is highly desirable to be able to assign the electronic transitions seen in the UV–vis spectrum of the singlet ground state.

In this paper we report the results of our *ab initio* calculations of the UV–vis spectrum of **TMB**. We have performed calculations that provide both π–π and σ–π correlation. The computed excitation energies from 1^1A_g, which the calculations find to be the ground state of **TMB**, give a very good account of the UV–vis spectrum that has been attributed to this diradical.[8,9] The calculations allow the identification of the long-wavelength absorption as belonging to the excitation from 1^1A_g to 2^1A_g.

* Abstract published in *Advance ACS Abstracts*, June 1, 1994.

(1) Borden, W. T.; Davidson, E. R. *J. Am. Chem. Soc.* **1977**, *99*, 4587.

(2) Reviews: (a) Borden, W. T. In *Diradicals*; Borden, W. T., Ed.; Wiley-Interscience: New York, 1982; pp 1–72. (b) Borden, W. T. *Mol. Cryst. Liq. Cryst.* **1993**, *232*, 195.

(3) (a) Lahti, P. M.; Rossi, A.; Berson, J. A. *J. Am. Chem. Soc.* **1991**, *113*, 2318. (b) Lahti, P. M.; Ichimura, A. S.; Berson, J. A. *J. Org. Chem.* **1989**, *54*, 958.

(4) Lahti, P. M.; Rossi, A.; Berson, J. A. *J. Am. Chem. Soc.* **1985**, *107*, 4362.

(5) Du, P; Hrovat, D. A.; Borden, W. T.; Lahti, P. M.; Rossi, A.; Berson, J. A. *J. Am. Chem. Soc.* **1986**, *108*, 5072.

(6) Hund, F. *Linienspektren Periodisches System der Elemente*; Springer-Verlag: Berlin, 1927; p 124ff. Hund, F. *Z. Phys.* **1928**, *51*, 759.

(7) Violations of Hund's rule in non-Kekulé molecules have been reviewed: Borden, W. T.; Iwamura, H.; Berson, J. A. *Acc. Chem. Res.* **1994**, *27*, 109.

(8) (a) Roth, W. R.; Langer, R.; Bartmann, M.; Stevermann, B.; Maier, G.; Reisenauer, H. P.; Sustmann, R.; Müller, W. *Angew. Chem., Int. Ed. Engl.* **1987**, *26*, 256. (b) Roth, W. R.; Langer, R.; Ebbrecht, T.; Beitat, A.; Lennartz, H.-W. *Chem. Ber.* **1991**, *124*, 2751.

(9) (a) Reynolds, J. H.; Berson, J. A.; Kumashiro, K. K.; Duchamp, J. C.; Zilm, K. W.; Rubello, A.; Vogel, P. *J. Am. Chem. Soc.* **1992**, *114*, 763. (b) Reynolds, J. H.; Berson, J. A.; Scaiano, J. C.; Berinstain, A. B. *J. Am. Chem. Soc.* **1992**, *114*, 5866. (c) Reynolds, J. H.; Berson, J. A.; Kumashiro, K. K.; Duchamp, J. C.; Zilm, K. W.; Scaiano, J. C.; Berinstain, A. B.; Rubello, A.; Vogel, P. *J. Am. Chem. Soc.* **1993**, *115*, 8073.

0002-7863/94/1516-6327$04.50/0

Computational Methodology

We began by optimizing the geometry of the lowest triplet state ($^3B_{1u}$) at the UHF level with the 6-31G* basis set.[10] Previous calculations have shown that the UHF optimized geometry of $^3B_{1u}$ is close to that of the π CI optimized geometry of not only this state but also the ^1A_g ground state.[5] We also optimized at the UHF/6-31G* level the geometry of the ^5A_g state, since we believed that this geometry would provide a good first approximation to the geometries of excited states to which structure B in Figure 1 makes a large contribution. These geometry optimizations were performed with the Gaussian 92 package of *ab initio* programs,[11] and the fully optimized geometries are available as Supplementary Material.

MCSCF calculations were performed that included all possible configurations of a given symmetry in which the ten π electrons are allowed to occupy the ten lowest energy π orbitals (4 bonding, 2 nonbonding, and four antibonding). These complete active space (CAS) SCF calculations not only provide correlation among the π electrons but also optimize the orbitals in the single-configuration wave function for the σ electrons in each state. The 10/10 CASSCF calculations proved too large for the MCSCF module in Gaussian 92, so they were performed with the program MOLCAS.[12]

Although calculations at the UHF/6-31G* geometry of $^3B_{1u}$ might be expected to provide reasonably good vertical excitation energies within both the singlet and triplet manifolds, in order to compute adiabatic excitation energies, the geometries of the excited states had to be optimized. Unfortunately, analytical energy gradients are not yet available in MOLCAS; so we had to resort to geometry optimizations, using single-point energy calculations. All C–H bond lengths and all bond angles were frozen at their UHF optimized values, and the three types of C–C bond lengths in **TMB** were optimized by fitting a series of CASSCF energies, calculated at ten different geometries, to a quadratic potential surface for each electronic state. The ^5A_g rather than the $^3B_{1u}$ optimized UHF geometry provided a better starting point for the CASSCF optimization of the geometry of the 2^1A_g excited state.

In order to include the effects of additional electron correlation, particularly between σ and π electrons, CASPT2N calculations were performed, again using MOLCAS. CASPT2N employs second-order perturbation theory to obtain the correlation energy for all the electrons in a molecule, starting from a MCSCF reference wave function.[13] CASPT2N is the multi-configurational equivalent of MP2,[14] to which it reduces for a reference wave function consisting of a single, closed-shell configuration. Calculations at the CASPT2N level of theory have been successful in obtaining good agreement between computed and observed excitation energies in some organic molecules.[15]

Results and Discussion

CASSCF Calculations. The results of the CASSCF calculations at the UHF optimized geometry of $^3B_{1u}$ are given in Table 1. The CASSCF singlet and triplet excitation energies are all about 0.5–0.7 eV lower than those computed previously by π SDTQ CI, using just 10 π MOs and only one or two reference configurations.[5] However, the energy difference between the lowest singlet and triplet is nearly unchanged; and the energy ordering of the excited states is also unaffected.

Table 1. CASSCF and CASPT2N/6-31G* Energies (eV) for the Low-Lying Singlet and Triplet States of **TMB** at the UHF/6-31G* Optimized Geometry for the $^3B_{1u}$ State

state	E(CASSCF)	E(CASPT2N)	state	E(CASSCF)	E(CASPT2N)
1^1A_g	0[a]	0[b]	$^3B_{1u}$	0.20	0.20
$^1B_{3u}$	2.89	2.48	$^3B_{3u}$	2.20	1.85
$^1B_{2g}$	3.26	2.94	$^3B_{2g}$	2.52	2.23
2^1A_g	3.28	2.44	^3A_g	3.78	3.44
$^1B_{1u}$	4.68	3.97	2^3B_{1u}	3.83	3.48

[a] Relative to E = –384.5108 hartrees. [b] Relative to E = –385.6993 hartrees.

As discussed previously,[5] the wave functions for the lowest singlet (1^1A_g) and triplet ($^3B_{1u}$) both resemble that for two pentadienyl radicals. Hence both states are reasonably well represented by structure **A** in Figure 1. However, in the lowest singlet the opposite spins of the electrons in the two pentadienyl NBMOs and of the electrons in the bonding π MOs that are polarized by these two electrons allow some π bonding between the carbons in different pentadienyl fragments. This bonding is not present in the lowest triplet state, which is why the singlet is calculated to be the ground state of **TMB**. Put in terms of the resonance structures in Figure 1, the singlet is the ground state of **TMB** because structure **B** makes a contribution to the wave function for this state, but not to the wave function for the lowest triplet.

The wave functions for the excited singlet ($^1B_{3u}$) and triplet ($^3B_{3u}$) states of **TMB** that are of lowest energy at the CASSCF level each consist of two dominant configurations. One of these represents the excitation of one electron from the out-of-phase combination of doubly occupied pentadienyl π HOMOs ($1a_u$) into the in-phase combination of pentadienyl NBMOs ($2b_{2u}$). The other involves the excitation of one electron from the out-of-phase combination of NBMOs ($2b_{3g}$) into the in-phase combination of pentadienyl LUMOs ($2b_{1g}$). These MOs are depicted schematically in Figure 2.

The $1^1A_g \rightarrow {}^1B_{3u}$ excitation is allowed and polarized along the long molecular axis of **TMB**. The $^3B_{1u} \rightarrow {}^3B_{3u}$ excitation is forbidden. However, the transition to B_{2g}, the excited state of next lowest energy in the CASSCF calculations, is forbidden in the singlet manifold, but allowed and polarized along the long molecular axis in the triplet.

The B_{2g} excited states also involve excitations among the same four orbitals as B_{3u}, but in B_{2g} the excitations are $1a_u \rightarrow 2b_{3g}$ in one electronic configuration and $2b_{2u} \rightarrow 2b_{1g}$ in another. The in-phase combination of pentadienyl NBMOs ($2b_{2u}$) is lower in energy than the out-of-phase combination ($2b_{3g}$), and this makes the excitations out of the former NBMO and into the latter in the B_{2g} excited states higher in energy than the excitations into $2b_{2u}$ and out of $2b_{3g}$ in the B_{3u} excited states. Therefore, there is little doubt that the MCSCF ordering of these two types of excited states is correct, so that the allowed transition to $^1B_{3u}$ is lower in energy than the forbidden transition to $^1B_{2g}$, and the forbidden transition to $^3B_{3u}$ is lower in energy than the allowed transition to $^3B_{2g}$.

Consequently, if both the MCSCF and previous π CI calculations[5] were correct in predicting that $^1B_{3u}$ and $^1B_{2g}$ are the first two excited singlet states, the experimental UV–vis spectrum, which shows a weak transition, followed by a much stronger one at higher energy,[8,9] could not belong to singlet **TMB**. However, as pointed out by Roth and co-workers,[8] the observed spectrum would fit that anticipated for triplet **TMB**. Therefore, if the UV–vis spectrum that is observed does, in fact, belong to 1^1A_g, the MCSCF and π CI calculations must be wrong. There must be another excited singlet state that is lower in energy than either $^1B_{3u}$ or $^1B_{2g}$ and that is responsible for the longest wavelength band in the UV–vis spectrum of **TMB**.

(10) Hariharan, P. C.; Pople, J. A. *Theor. Chim. Acta* **1973**, *28*, 213.
(11) Frisch, M. J.; Trucks, G. W.; Head-Gordon, M.; Gill, W. P. M.; Wong, M. W.; Foresman, J. B.; Johnson, B. G.; Schlegel, H. B.; Robb, M. A.; Replogle, E. S.; Gomperts, R.; Andres, J. L.; Raghavachari, K.; Binkley, J. S.; Gonzalez, C.; Martin, R. L.; Fox, D. J.; Defrees, D. J.; Baker, J.; Stewart, J. J. P.; Pople, J. A.; Gaussian, Inc.: Pittsburgh, PA, 1992.
(12) Andersson, K.; Blomberg, M. R. A.; Fülscher, M. P.; Kellö, V.; Lindh, R.; Malmqvist, P.-A.; Noga, J.; Olsen, J.; Roos, B. O.; Sadlej, A. J.; Siegbahn, P. E. M.; Urban, M.; Widmark, P.-O. MOLCAS, Version 2, University of Lund, Sweden 1991.
(13) Andersson, K.; Malmqvist, P.-A.; Roos, B. O. *J. Chem. Phys.* **1992**, *96*, 1218. In a subsequent paper, which discusses some applications, this method has been referred to as CASPT2F: Andersson, K.; Roos, B. O. *Int. J. Quantum Chem.* **1993**, *45*, 591.
(14) Moller, C.; Plesset, M. S. *Phys. Rev.* **1934**, *46*, 618. Pople, J. A.; Binkley, J. S.; Seeger, R. *Int. J. Quantum Chem.* **1976**, *S10*, 1.
(15) Serrano-Andrés, L.; Merchán, M.; Nebot-Gil, I.; Roos, B. O.; Fülscher, M. *J. Am. Chem. Soc.* **1993**, *115*, 6184.
(16) (a) Buenker, R. J.; Peyerimhoff, S. D. *J. Chem. Phys.* **1968**, *48*, 354. (b) Borden, W. T.; Davidson, E. R.; Hart, P. *J. Am. Chem. Soc.* **1978**, *100*, 388. (c) Jafri, J. A.; Newton, M. *J. Am. Chem. Soc.* **1978**, *100*, 5012. (d) Agren, H.; Correia, N.; Flores-Riveros, A.; Jensen, H. J. A. *Int. J. Quantum Chem.* **1986**, *19*, 237. (e) Nakamura, K.; Osamura, Y.; Iwata, S. *Chem. Phys.* **1989**, *136*, 67.

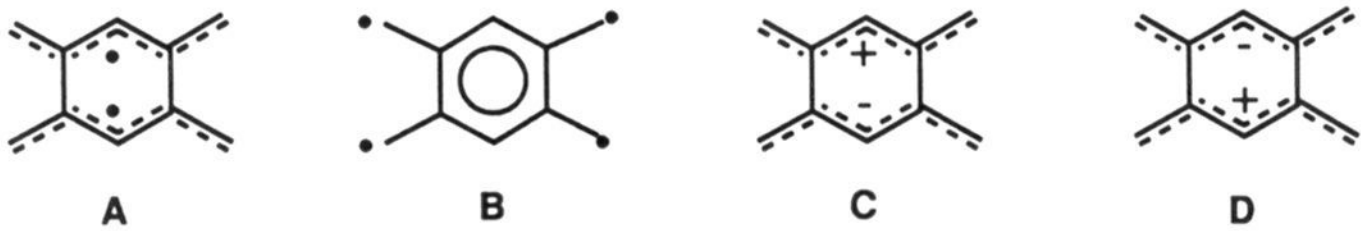

Figure 1. Some covalent and ionic resonance structures for **TMB**.

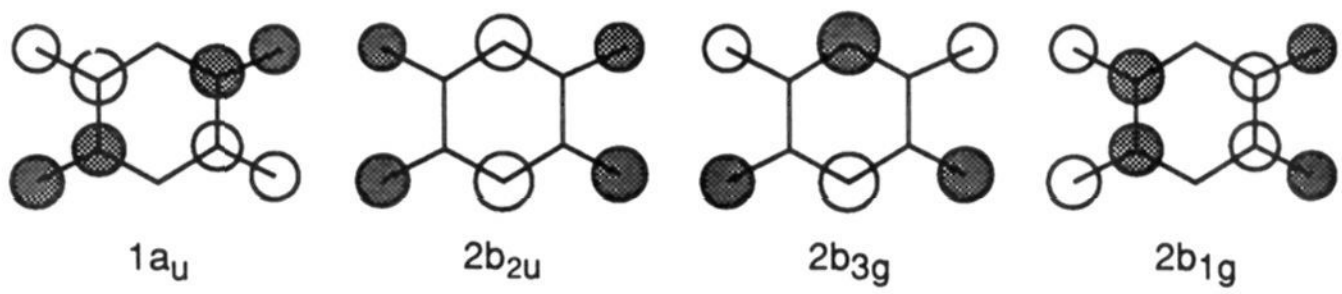

Figure 2. Schematic depiction of the doubly occupied HOMO ($1a_u$), the two NBMOs ($2b_{2u}$ and $2b_{3g}$), and the LUMO ($2b_{1g}$) of **TMB**. Only one lobe of each of the p AOs that constitute these π MOs is shown.

CASPT2N Calculations. The CASPT2N results in Table 1 suggest that this might, indeed, be the case. Although the CASPT2N excitation energies from 1^1A_g to $^1B_{3u}$ and $^1B_{2g}$ are respectively 0.41 and 0.32 eV lower than those computed at the CASSCF level, the excitation energies to 2^1A_g and $^1B_{1u}$ decrease by respectively 0.84 and 0.71 eV on going from the CASSCF to the CASPT2N level of theory. As shown in Table 1, the 0.43 eV larger drop in 2^1A_g than in $^1B_{3u}$ makes these two excited states nearly isoenergetic at the CASPT2N level of theory.

The selective stabilization of 2^1A_g and $^1B_{1u}$ at the CASPT2N level, relative to the three other singlet states, is readily explained. Like the 1^1A_g ground state, the zeroth-order wave functions for these two excited states place a total of two electrons in the two NBMOs. However, the 1^1A_g wave function, $|...2b_{2u}^2\rangle - |...2b_{3g}^2\rangle$, results in these two electrons being confined to different pentadienyl fragments, so that they never appear simultaneously in the same AO. In contrast, the 2^1A_g wave function, $|...2b_{2u}^2\rangle + |...2b_{3g}^2\rangle$, and the $^1B_{1u}$ wave function, $|...2b_{2u}2b_{3g}(\alpha\beta - \beta\alpha)\rangle$, both confine these electrons to the same pentadienyl fragment.[2a] Thus, although structure **A** in Figure 1 provides a reasonable representation of 1^1A_g, the in-phase and out-of-phase combinations of structures **C** and **D** provide depictions of the zeroth-order MO wave functions for respectively 2^1A_g and $^1B_{1u}$.

The highly ionic character of 2^1A_g and $^1B_{1u}$ explains why their energies are calculated to be much higher than that of 1^1A_g. Their highly ionic character also explains why they are significantly stabilized, relative to 1^1A_g, on going from the CASSCF to the CASPT2N level of theory. Providing correlation between the σ and π electrons allows the former to help stabilize ionic terms in the wave functions for the latter. Put crudely, correlating the σ and π electrons allows dipoles created by the σ electrons to help stabilize the dipoles of opposite sign that are created by the π electrons.

Because the NBMOs of **TMB** are disjoint, using the zeroth-order wave functions, $2^1A_g = |...2b_{2u}^2\rangle + |...2b_{3g}^2\rangle$ and $^1B_{1u} = |...2b_{2u}2b_{3g}(\alpha\beta - \beta\alpha)\rangle$, the 2^1A_g and $^1B_{1u}$ excited states would be calculated to have almost exactly the same energies.[2a] However, the results in Table 1 show that at the CASSCF (and CASPT2N) level of theory 2^1A_g lies below $^1B_{1u}$ by 1.40 (1.53) eV. It is apparent that π electron correlation must selectively stabilize 2^1A_g.

The 2^1A_g State. The stabilization of 2^1A_g, relative to $^1B_{1u}$, by π electron correlation in **TMB** has a parallel in the stabilization of the $^1A_{1g}$ relative to the $^1B_{2g}$ excited state in square (D_{4h}) cyclobutadiene (**CBD**),[16] another disjoint diradical.[1,2,7] Mulder has explained this result in **CBD** by pointing out that in valence bond (VB) theory there are two singlet wave functions that allow four electrons to occupy four separate atomic orbitals.[17] One of these corresponds to the spin coupling in the $^1B_{1g}$ ground state of D_{4h} **CBD** and the other to the spin coupling in the $^1A_{1g}$ excited state. Thus, with inclusion of sufficient π electron correlation, the excited $^1A_{1g}$ state of **CBD**, which corresponds to the 2^1A_g excited state of **TMB**, can divest itself of all of its ionic terms and have the same electron repulsion energy as the $^1B_{1g}$ ground state.[18] In contrast, no amount of electron correlation can remove all the ionic terms from the wave function for the $^1B_{2g}$ excited state of **CBD**, the state which corresponds to the $^1B_{1u}$ excited state of **TMB**.

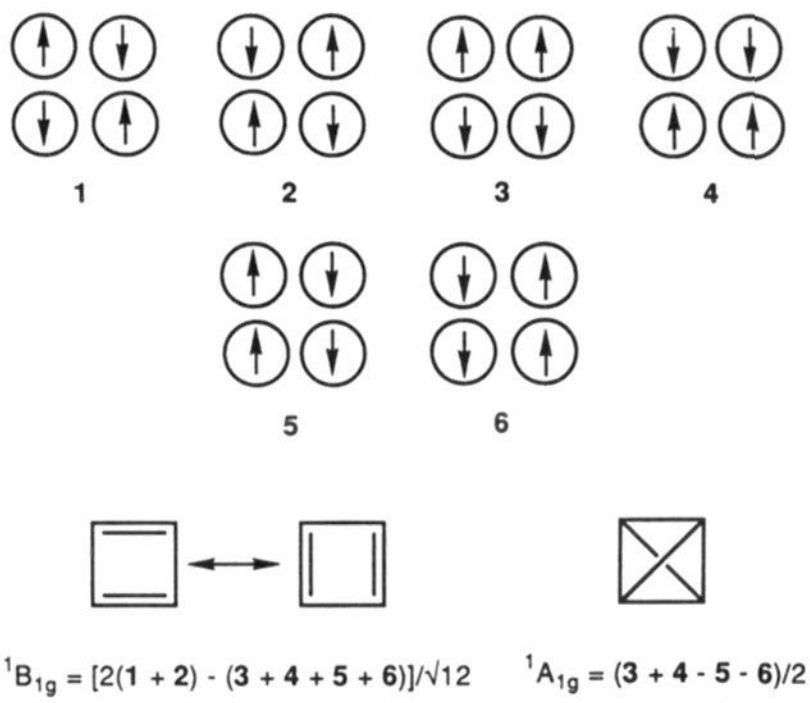

Figure 3. Graphical depiction of the six possible spin couplings for four electrons in four orbitals with $S_z = 0$. Different linear combinations of these give one quintet, three triplet, and two singlet states. The linear combinations that give the two lowest singlet states of **CBD** are shown.

In order to understand better the nature of the 2^1A_g state of **TMB**, it is useful to examine from a VB perspective the two singlet wave functions for four electrons in four separate, but identical, AOs. The possible spin couplings of the electrons with $S_z = 0$ are depicted graphically in Figure 3. The linear combinations of spin couplings that give the two lowest singlet states of **CBD** are shown.

In VB theory, exchange of electrons of opposite spin between two AOs results in bonding. It is thus quite easy to see from inspection of the spin couplings in Figure 3 that in square **CBD** the $^1B_{1g}$ wave function results in π bonding between adjacent AOs. In contrast, in the $^1A_{1g}$ state π bonding takes place between AOs that are diagonally across the four-membered ring. It is for this reason that in VB theory $^1B_{1g}$ is predicted to be lower in energy than $^1A_{1g}$ in D_{4h} **CBD**.[18]

As its name implies, the π system of **TMB** can be conceptualized as consisting of the π electrons on the carbons of four methylene groups interacting with the π electrons of a central benzene ring. The dominant spin couplings in the VB wave function for the

(17) Mulder, J. J. C. *Nouv. J. Chim.* **1980**, *4*, 283.

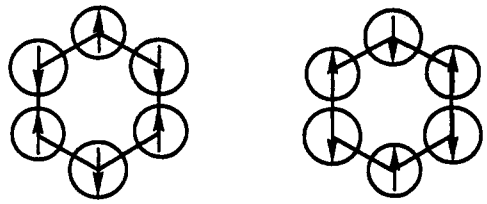

Figure 4. Graphical depiction of the dominant spin couplings in the π system of the ground state of benzene. Only one lobe of each of the p AOs that constitute the π system of benzene is shown.

ground state of benzene are shown in Figure 4; the other spin couplings can be derived from these two by exchanging pairs of α and β spin electrons.

Pairwise exchange of electrons of opposite spin between **3** in Figure 3 and the first structure in Figure 4 (as well as between **4** in Figure 3 and the second structure in Figure 4) gives π bonding between the four methylenes and the central benzene ring. When the π bonding due to pairwise exchange of the α and β spin electrons within the benzene ring is also considered, a hybrid of structures **A** and **B** in Figure 1 is obtained. In VB theory these structures represent the bonding in the lowest singlet state of **TMB**.[19]

A 4-fold symmetry axis is absent in **TMB**, and both singlet wave functions for four electrons in four different AOs have ^1A_g symmetry in the D_{2h} point group to which **TMB** belongs. If **3** and **4** in Figure 3 are the dominant spin couplings in the singlet VB wave function for the π electrons on the four methylene groups in the 1^1A_g ground state of **TMB**, the singlet wave function for these four electrons in the 2^1A_g excited state is $2^1A_g = (1 + 2 - 5 - 6)/2$.[20]

None of the spin couplings in this VB wave function of the four π electrons on the four methylene groups in **TMB** allow bonding with the π electrons in the VB wave function for the central benzene ring. Consequently, to the extent that electron correlation divests the π wave function for the 2^1A_g excited state of ionic terms so that it approaches the VB limit, the π bonding in this singlet state of **TMB** will resemble that in structure **B** of Figure 1.[21]

Calculations at Optimized Geometries. Since 2^1A_g is expected to contain an appreciable contribution from structure **B**, as well as from ionic structures **C** and **D**, the C–C bond lengths in the 2^1A_g excited state should be very different from those in the 1^1A_g ground state. Therefore, we optimized the C–C bond lengths of these two singlet states, as well as those of $^1B_{3u}$, the other low-lying excited singlet state, and of $^3B_{1u}$, the lowest triplet state. The optimized C–C bond lengths in these four states of **TMB** and their CASSCF and CASPT2N energies are given in Table 2.

Table 2. C–C Bond Lengths (Å) and CASSCF and CASPT2N/6-31G* Energies (eV) at CASSCF/6-31G* Optimized Geometries for Some Low-Lying States of **TMB**

state	$R(C_1–C_2)$	$R(C_2–C_3)$	$R(C_1–CH_2)$	E(CASSCF)	E(CASPT2N)
1^1A_g	1.483	1.422	1.377	0[a]	0[b]
$^3B_{1u}$	1.493	1.424	1.375	0.22	0.22
$^1B_{3u}$	1.482	1.426	1.397	2.82	2.41
2^1A_g	1.421	1.407	1.448	2.62	2.27
2^1A_g[c]	1.418	1.414	1.438		2.22

[a] Relative to $E = -384.5121$ hartrees. [b] Relative to $E = -385.7009$ hartrees. [c] Geometry optimized with CASPT2N/6-31G* calculations.

The CASSCF optimized C–C bond lengths in the 1^1A_g ground state are similar to those [$R(C_1–C_2) = 1.513$ Å, $R(C_2–C_3) = 1.418$ Å, and $R(C_1–CH_2) = 1.370$ Å] obtained by the UHF calculations on $^3B_{1u}$. The two geometries are so similar that both their CASSCF and their CASPT2N energies differ by less than 1 kcal/mol.

As found also by previous π CI calculations,[5] the CASSCF optimized C–C bond lengths of $^3B_{1u}$ are nearly the same as those of 1^1A_g. The biggest difference is that of 0.010 Å between the lengths of the $C_1–C_2$ ($C_4–C_5$) bonds that join the two pentadienyl fragments. This bond length is shorter in the singlet than in the triplet, because the opposite spins of the electrons in the NBMOs in the singlet allow some π bonding between these carbons in the singlet that is not possible in the triplet. The contribution of structure **B** in Figure 1 to the singlet, but not to the triplet, can be understood on the basis of either MO[5] or VB[19] theory.

The biggest difference between the C–C bond lengths of 1^1A_g and the $^1B_{3u}$ excited state is the 0.020 Å greater length of the bonds to the exocyclic methylene groups in the excited state. As discussed above, in the excited state electrons are excited from symmetry combinations of the HOMOs of the two pentadienyls ($1a_u$ and, to a lesser extent, $1b_{1g}$) into the NBMOs and from the NBMOs into symmetry combinations of the pentadienyl LUMOs ($2b_{1g}$ and, to a lesser extent, $2a_u$). The HOMO and LUMO of each of the pentadienyl moieties in **TMB** have nodes at C_3 and C_6, so that the bond lengths most affected by these excitations are those between the remaining four ring carbons and the exocyclic methylene groups attached to them.

As expected from the discussion in the previous section, the CASSCF geometry for the 2^1A_g excited state has very different C–C bond lengths than the geometry for the 1^1A_g ground state. In 2^1A_g the C–C bond lengths in the six-membered ring are more nearly equal and those to the exocyclic carbons are much longer than in 1^1A_g, indicating, as anticipated, a much larger contribution from structure **B** in the excited state than in the ground state. The CASSCF C–C bond lengths in 2^1A_g are much closer to the UHF bond lengths in ^5A_g [$R(C_1–C_2) = 1.405$ Å, $R(C_2–C_3) = 1.393$ Å, and $R(C_1–CH_2) = 1.464$ Å] than to the C–C bond lengths in the 1^1A_g ground state.

Because the optimized geometries of $^3B_{1u}$ and $^1B_{3u}$ are similar to those of 1^1A_g, bond length optimization has very little effect on the relative energies of these three states. However, because the optimized geometry of 2^1A_g is very different than that of 1^1A_g, there is a very significant effect of bond length optimization on the energy of 2^1A_g, relative to the energies of both 1^1A_g and $^1B_{3u}$. At the CASSCF level, bond length optimization decreases the excitation energy from 1^1A_g to 2^1A_g by 0.66 eV. The 0.59 eV change in the relative CASSCF energies of $^1B_{3u}$ and 2^1A_g results in 2^1A_g falling 0.20 eV below $^1B_{3u}$ after bond length optimization.

At the CASPT2N level of theory bond length optimization has a much less dramatic effect than at the CASSCF level on changing the energy of 2^1A_g, relative to the other low-lying states of **TMB**. Bond length optimization decreases the CASPT2N

(18) VB theory emphasizes electron correlation, so that simple VB wave functions contain no ionic terms.[2b] Consequently, in VB theory the $^1B_{1g}$ and $^1A_{1g}$ states of D_{4h} **CBD** have the same electron repulsion energy. However, as depicted in Figure 3, the former state has π bonding between adjacent carbon atoms and the latter only between atoms diagonally across the ring. Therefore, in VB theory $^1B_{1g}$ has more π bonding than $^1A_{1g}$ and, hence, is the lower energy state. In contrast, the zeroth order MO wave functions for the $^1B_{1g}$ and $^1A_{1g}$ states of D_{4h} **CBD** have the same amount of π bonding, since the same set of MOs is occupied in both states. However, the former wave function has a much lower electron-repulsion energy than the latter, so that in simple MO theory $^1B_{1g}$ is also predicted to be the lower energy of the two states. Therefore, whether one begins by assuming equal electron repulsion energies, as in VB theory, or equal amounts of π bonding, as in simple MO theory, $^1B_{1g}$ is predicted to be lower in energy than $^1A_{1g}$.

(19) In VB theory the $S_z = 1$ component of the lowest triplet state ($^3B_{1u}$) of **TMB** can be thought of as resulting from coupling of the $S_z = 2$ quintet state of the four π electrons on the methylene groups with the $S_z = -1$ component of the triplet state of benzene that resembles two allyl radicals with parallel spins. Consequently, unlike the lowest singlet (^1A_g), in VB theory the triplet has no contribution from structure B and, hence, is slightly higher in energy than the singlet.

(20) The two singlet VB wave functions for the π electrons of the four methylene groups in **TMB** are orthonormal linear combinations of the two singlet VB wave functions for the π electrons in **CBD**, which are given in Figure 3.

(21) The electronic structure of 2^1A_g is expected to be a hybrid of resonance structures **B–D**. Therefore, whether π bonding is maximized or electron repulsion is minimized in this state, 1^1A_g, which can be represented by structure **A** plus a small contribution from **B**, is predicted to be the state of lower energy. The situation is analogous to that with the $^1B_{1g}$ and $^1A_{1g}$ states in **CBD**.[18]

$1^1A_g \rightarrow 2^1A_g$ excitation energy by only 0.17 eV and lowers the energy of 2^1A_g, relative to $^1B_{3u}$, by just 0.10 eV. Nevertheless, since the CASPT2N energy of 2^1A_g is slightly lower than that of $^1B_{3u}$ before bond length optimization, after optimization of the C–C bond lengths 2^1A_g drops below $^1B_{3u}$ by 0.14 eV at the CASPT2N level of theory.

The difference between the effect of C–C bond length optimization on the CASSCF and CASPT2N energies of 2^1A_g is almost certainly related to the schizophrenic nature of this excited state, which is a hybrid of structures **B**, **C**, and **D** in Figure 1. The lack of σ–π electron correlation at the CASSCF level tends to accentuate the importance of structure **B**, relative to ionic structures **C** and **D**, at this level of theory. Consequently, since it is the contribution of structure **B** to the wave function for 2^1A_g that causes this excited state to prefer a very different geometry than the other three low-lying states, C–C bond length optimization has a large effect on the relative energy of 2^1A_g at the CASSCF level. However, since σ–π electron correlation is included at the CASPT2N level, the importance of **B**, relative to **C** and **D**, decreases at this level, so that bond length optimization has a smaller effect on the energy of 2^1A_g at the CASPT2N level than at the CASSCF level.

Different weights for structure **B**, relative to **C** and **D**, in the CASSCF and CASPT2N wave functions for 2^1A_g could, in principle, result in rather different optimized geometries for this state at these two levels of theory. Therefore, we reoptimized the C–C bond lengths of 2^1A_g at the CASPT2N level of theory. As shown in Table 2, the CASSCF and CASPT2N optimized geometries for this state do differ slightly, but the difference in the CASPT2N energies at these two geometries amounts to only about 1 kcal/mol.

Comparison with Experiment. The results given in Table 2 provide strong evidence that 2^1A_g is the excited state responsible for the longest wavelength absorption observed[8,9] in the UV–vis spectra of **TMB**. The calculations show that 2^1A_g has three qualitative features that fit this band, which is (1) weak, (2) shows a large amount of vibrational structure, and (3) occurs at only slightly longer wavelengths than a strong absorption that appears to have much less vibrational structure. First, the $1^1A_g \rightarrow 2^1A_g$ transition is forbidden, so that this excitation should produce a weak absorption.[22] Second, since these two states are calculated to have rather different C–C bond lengths, the $1^1A_g \rightarrow 2^1A_g$ excitation should produce an absorption that has vibrational structure, caused by population of different energy levels of those a_g vibrational modes in the excited state that change the C–C bond lengths. Third, the calculations find that the adiabatic energy of the 2^1A_g excited state is close to, but lower than, that of $^1B_{3u}$. The excitation from the 1^1A_g ground state to $^1B_{3u}$ represents an allowed transition; and because these two states are calculated to have rather similar geometries, the strong absorption that corresponds to this transition should have less vibrational structure than the weak absorption that corresponds to $1^1A_g \rightarrow 2^1A_g$.

Although the geometries of the $^1B_{2g}$ and the $^1B_{1u}$ excited states have not been optimized, the CASPT2N energies of these two states in Table 1 suggest that the very weak absorption around 400 nm (3.1 eV) in the UV–vis spectrum of **TMB** corresponds to the forbidden $1^1A_g \rightarrow {}^1B_{2g}$ transition and that the strong band that begins around 330 nm (3.8 eV) corresponds to the allowed $1^1A_g \rightarrow {}^1B_{1u}$ excitation. The CASPT2N excitation energies in Table 1 that are calculated for these two transitions are both higher than those measured, but only by about 0.2 eV. Optimization of the geometries of the excited states would probably bring the calculated excitation energies into even better agreement with those observed.

The adiabatic CASPT2N excitation energies calculated for the two lowest energy transitions in **TMB** are also in very good quantitative agreement with the position of the two longest wavelength bands in the UV–vis spectrum of this diradical. The strong absorption with $\lambda_{max} = 475$ nm in argon[8] (490 nm in frozen organic solutions)[9] corresponds to an excitation energy of 2.6 eV. The agreement with the calculated CASPT2N excitation energy of 2.41 eV in Table 2 for the allowed $1^1A_g \rightarrow {}^1B_{3u}$ excitation is good and would be even better if the shoulder observed at 510 nm (2.4 eV) corresponds to the transition to the lowest vibrational level of the excited state.

The weak absorption at longest wavelength, which terminates at slightly above 600 nm in argon[8] (620 nm in frozen solutions),[9] corresponds to an adiabatic excitation energy of 2.1 eV. This is a bit lower than the value of 2.22 eV computed for the CASPT2N optimized geometry of 2^1A_g. However, it should be noted that the ^5A_g state, to which 2^1A_g bears some resemblance, has a UHF zero-point vibrational energy that is 0.13 eV lower than that of $^3B_{1u}$, in which the bonding is similar to that in 1^1A_g.[23] To the extent that 2^1A_g has a lower vibrational energy than 1^1A_g, the calculated adiabatic excitation energy will be lower than that given in Table 2 and in even better agreement with experiment.

The close agreement of the UV–vis spectrum observed for **TMB** with that calculated at the CASPT2N level for the lowest singlet state leaves little doubt that the observed spectrum has its origin in this state. Both the higher energy computed at all levels for $^3B_{1u}$, relative to 1^1A_g, and the much poorer agreement between the observed spectrum and the CASPT2N excitation energies computed for the triplet manifold (Table 1)[24] provide no support for a triplet ground state for **TMB**. Therefore, the results of the CASPT2N calculations reported here show that the observed UV–vis spectrum of **TMB**[8,9] provides an additional piece of experimental evidence that, as predicted,[3-5] this diradical has a singlet ground state[9] and thus violates Hund's rule.[6,7]

Acknowledgment. We thank the National Science Foundation for support of this research and Professor Berson for his persistence in challenging us to identify the state responsible for the long-wavelength absorption in the UV–vis spectrum of **TMB**.

Supplementary Material Available: Listing of UHF/6-31G* optimized geometries for the $^3B_{1u}$ and ^5A_g states of **TMB** (1 page). This material is contained in many libraries on microfiche, immediately follows this article in the microfilm version of the journal, and can be ordered from the ACS; see any current masthead page for ordering information.

(22) The transition to the 2^1A_g excited state can "borrow intensity" by vibrational mixing with the energetically proximate $^1B_{3u}$ excited state. The two states can be mixed by b_{3u} vibrations, which asymmetrically distort **TMB** along the long molecular axis. Excitation of one or more b_{3u} vibrations in the 2^1A_g excited state may also contribute to the vibrational structure that is seen in the longest wavelength absorption of **TMB**.

(23) The lower vibrational energy of ^5A_g has its origin in the weaker π bonding (greater contribution from structure **B** in Figure 1) in this state than in $^3B_{1u}$.

(24) For example, the forbidden $^3B_{1u} \rightarrow {}^3B_{3u}$ absorption is calculated to occur around 750 nm, which is far to the red of where the weak absorption in the UV–vis spectrum of **TMB** is observed.